Journal of Advanced Joining Processes 1 (2020) 100012

Contents lists available at ScienceDirect

Journal of Advanced Joining Processes

journal homepage: www.elsevier.com/locate/jajp

New approaches on laser micro welding of copper by using a laser beam source with a wavelength of 450 nm

Marc Hummel[a,*], Christoph Schöler[b], André Häusler[c], Arnold Gillner[a,c], Reinhart Poprawe[a,c]

[a] Chair for Laser Technology LLT, RWTH Aachen University, Steinbachstraße 15, 52074 Aachen, Germany
[b] Nonlinear Dynamics of Laser Processing NLD, RWTH Aachen University, Steinbachstraße 15, 52074 Aachen, Germany
[c] Fraunhofer-Institute for Laser Technology ILT, Steinbachstraße 15, 52074 Aachen, Germany

ARTICLE INFO

Keywords:
Laser micro welding
450 nm
Heat conduction welding
Copper
Scanner system
Modeling

ABSTRACT

Laser micro welding is specified with welding geometries below 1 mm and is used with increasing demand for contacting electronic components such as battery and fuel cells. Fiber lasers with a wavelength in the near infrared range (IR, $\lambda \approx 1$ µm) have established themselves for this purpose. The laser welding process allows processing of parts in the micron range but reduces the surface quality of the processed parts at the same time. Furthermore, weld defects can occur due to process instabilities caused by the low absorptivity (<5%) of copper for infrared radiation. Therefore, alternative laser beam sources and processes have to be established, to avoid these negative effects on the weld seam quality. Laser beam sources in the visible wavelength range (VIS) prove to be an alternative due to an increased absorption of the laser energy in copper-based alloys.

This paper presents the observation of laser micro welding of Cu-ETP and CuSn6 specimen with a thickness between 150 µm and 1 mm. The diode laser is specified by a wavelength of 450 nm and a nominal output power of 150 W. The surface roughness of the weld seam and the overall weld seam geometry for heat conduction welding are investigated. The laser energy absorption is measured using two integrating spheres to compare the results quantitatively to measurements conducted with laser sources of 1070 nm and 515 nm. For detailed observation high speed imaging is used to observe the melt pool dynamics. Simulations are conducted, to optimize the dimensioning of optics and laser beam source. Finally, the possible use of the novel laser beam source for various technical joining applications is discussed and evaluated and the influence of the use of protective gas is observed.

Introduction

In the production of electro mobility components, laser material processing is one of the key technologies for achieving sophisticating goals while ensuring high quality standards for the electrical and mechanical connection. Laser beam sources are used for cutting materials, manufacturing cell housings and welding conductor materials to battery cells. Cylindrical battery cells consist of a 250 µm battery housing while connector materials range between 100 and 300 µm thickness for standard applications (Mehlmann, 2014). For welding these materials with short processing times for minimized energy input, fiber laser beam sources with a wavelength in the near infrared range (1030–1070 nm) are in the focus of development. In this wavelength range, the degree of absorption of the laser radiation for the copper materials used for electrical contacting is below 5%. By developing laser beam sources in the range of the blue wavelength (450 nm), absorptivity up to 50–60% at ambient conditions becomes available for the process (Balck et al., 2018). This circumstance enables the development of more precise and controllable processes than before (Zediker, 2018).

There are currently investigations on the use and development of blue laser beam sources. The development of a laser beam source with sufficient laser power for laser beam micro welding in the range of 250 W and a wavelength of 450 nm was first published in 2017 (Wang et al., 2017). Subsequently, the AO-150 was developed by Nuburu Inc., which is the first commercially available diode laser with a wavelength of 450 nm and an output power of 150 W. First investigations on copper foils with a thickness of 125 µm show that copper can be welded without splashes and pores using the blue laser beam source (Zediker, 2018). Also in heat conduction welding, the formation of pores can be avoided (Finuf et al., 2017). Laser beam sources with higher laser power of up to 1.5 kW and improved beam quality are already the focus of development (Balck et al., 2018; Zediker, 2018; Baumann et al., 2019).

* Corresponding author.
E-mail address: marc.hummel@llt.rwth-aachen.de (M. Hummel).

https://doi.org/10.1016/j.jajp.2020.100012
Received 13 November 2019; Received in revised form 24 February 2020; Accepted 24 February 2020
2666-3309/© 2020 The Author(s). Published by Elsevier B.V. This is an open access article under the CC BY-NC-ND license.
(http://creativecommons.org/licenses/by-nc-nd/4.0/)

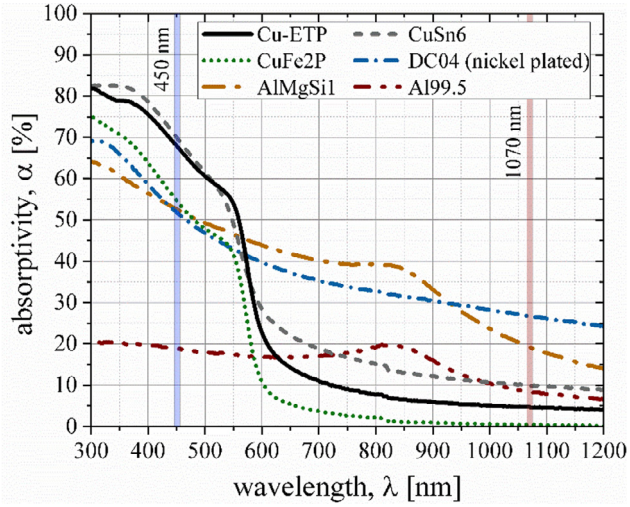


Fig. 1. Wavelength dependent absorptivity of different metal alloys from 300 nm to 1200 nm at ambient conditions.

Laser systems still under development and with an output power of > 500 W achieve a welding depth > 300 µm for bead-on-plate welds with a feed rate of 4 m/min (Zediker, 2019). All conducted investigations have in common that they use fixed optics with a high speed axis moving the material sample through the laser beam.

In the present work the laser system AO-150 from the company Nuburu Inc. with a wavelength of 450 nm is used for the investigations. Different to the previously mentioned publications the laser is implemented within a scanner based optical setup. Welding on Cu-ETP and CuSn6 is conducted with a profound analysis of the laser absorption during the process. High-speed videography is used to break down the process down into individual steps to analyze the process on the material surface. Technically important joint configurations such as butt and overlap joints are investigated to explore the limitations of a scanner application with the used laser beam source. The investigations are supported using a heat conduction model to classify the laser beam sources and give a roadmap for future applications of the 450 nm wavelength.

Theoretical background

To describe the absorption of electromagnetic waves on the surface of metallic materials on theoretical basis, many internal processes of the material have to be considered. Although a qualitative description of the electric properties can already be obtained from the simple Drude model in practice, however, the exact calculation of the absorption is only possible to a limited extent, since influences such as the geometric properties and the chemical composition of the surface has to be known accurately.

For the determination of the wavelength dependent absorptivity of different materials, an experimental procedure is necessary. The values shown in Fig. 1 are measured with a PerkinElmer Lambda 1050 UV/Vis Spectrophotometer.

They represent the absorptivity of the material at ambient temperature and in solid state. The properties of the measured materials are listed in Table 1.

For all investigated metallic materials the absorptivity increases with decreasing wavelength. For Cu-ETP the absorptivity increases from 2.5% at 1070 nm wavelength to 68% at 515 nm. The same behavior is observed for CuSn6. Here the absorptivity increases from 9.5% to 70%. The increase for aluminum is also observed but flatter than for the copper materials. Here the maximum absorptivity is about 24% at a wavelength of 808 nm. Since the wavelength continues to decrease, the absorption coefficient does not increase further. For aluminum alloys a significant increase can be observed such as AlMgSi1. The curves in Fig. 1 show, that especially in welding applications between copper and copper alloys, the use of laser beam sources with a wavelength in the range of 450 nm leads to a higher absorptivity during the welding process.

Table 1
Surface roughness and thermal conductivity of measured alloys (Moeller and Moeller, 2014).

Material	Surface roughness R_a	Thermal conductivity
Unit	[µm]	[W/m*K]
Cu-ETP	3.92	>393
CuSn6	3.29	75
CuFe2P	1.69	262
DC04 (n.p.)	3.04	45–55
Al99,5	3.23	215
AlMgSi1	1.16	167

Table 2
Properties of Nuburu AO-150.

Parameter	Unit	Magnitude
Wavelength	[nm]	450
Max. laser power	[W]	150
Fiber diameter	[µm]	200
BPP	[mm mrad]	< 15
Max. pulse duration	[s]	cw

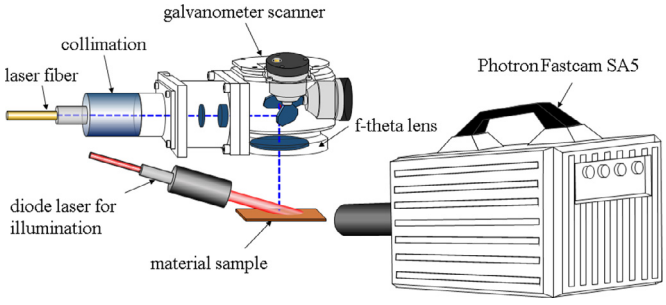


Fig. 2. Optical setup including high-speed videography.

Table 3
Properties of optical components.

Optical parameter	Unit	Magnitude
Focal length collimation	[mm]	45
Raw beam diameter	[mm]	20
Optical aperture scanner	[mm]	20
Focal length f-theta lens	[mm]	173
Theoretical focal diameter	[µm]	768

Experimental setup

For the experimental setup, a Nuburu AO-150 diode laser beam source with a wavelength of 450 nm is used. The properties of the laser beam source are listed in Table 2. Within this work, two different laser power levels will be used. An output power of 147.7 W is available after the focusing lense. Inside the experimental setup of the integrating spheres an laser power of 131.7 W is available on the material surface (89.14% transmittance of the beam splitter). The following investigations will be conducted with this maximum laser power.

Due to the laser properties, heat conduction welding with a scanner based system is performed. A Newson z-Shifter and a Galvanometer scanner are used to perform the laser welding on the material surface. A Scanlab f-theta lens is used to focus the laser beam onto the surface. The schematic representation of the setup is shown in Fig. 2.

To focus the laser beam on the surface, the optical components are used as follows in Table 3.

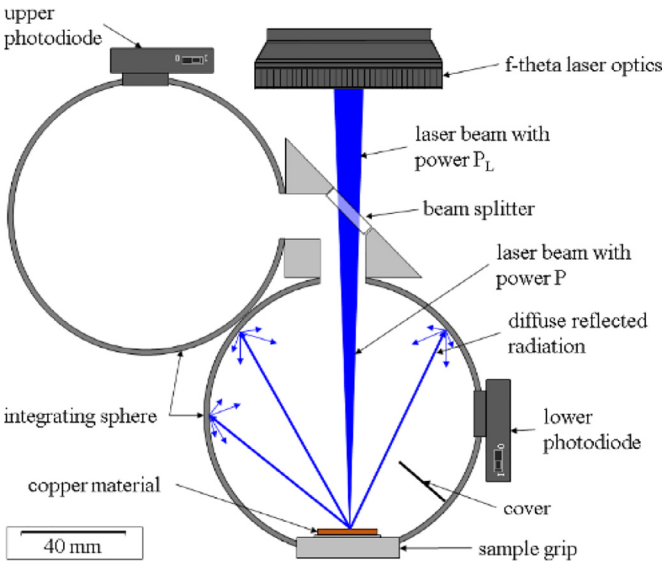


Fig. 3. Experimental setup of the integrating spheres.

The welding process is additionally observed with a Photron Fastcam SA5. The high speed-videography allows the detailed observation of the process dynamics. The setup is equipped with a diode laser radiating at 808 nm for process illumination. An optical broadband filter for 808 nm is used on the high-speed camera. The welded material samples are additionally observed by the preparation of cross sections. The bead-on-plate welds are conducted on specimens of Cu-ETP and CuSn6 with a dimension of 10 × 30 mm and a thickness of 1 mm. Further joining configurations are performed on material with thicknesses of 0.5 mm, 0.3 mm and 0.15 mm.

To determine the degree of absorptivity during the laser process, the reflected laser power is observed with two integrating spheres, as shown in Fig. 3. The material sample is placed inside the lower integrating sphere (819C-SF-4, Newport Corporation). Due to the position, the diffusely reflected radiation can be measured with the lower photodiode. The coaxial reflected radiation is deflected via a beam splitter (Thorlabs BSN10) in the upper integrating sphere (819D-SF-4, Newport Corporation). The beam splitter has a transmission of 89.14% and a reflectivity of 10.86%. The measurements in the two integrating spheres are performed with Si-photodiodes (Thorlabs DET100A/M). Both photodiodes are equipped with a bandpass filter (Thorlabs FL450-10) for noise suppression. With optical filters of known density (Thorlabs NEK01) the measurement signals at the photodiodes are further reduced in case of signal overload. The two signals are monitored using an InfiniiVision DSO-X 2002A oscilloscope from Agilent Technologies. All open ports in the integrating sphere have a diameter of 25.4 mm.

To assign a respective laser power to a measured photodiode signal, a calibration was conducted before the measurements. After a calibration measurement with a broadband mirror (Thorlabs BB05-E02) tilted by 8° the diode voltage of the lower photodiode can be assigned to a specific laser power. In order to take into account the radiation reflected vertically from the lower integrating sphere into the upper integrating sphere during the welding process, the diode voltage of the upper photodiode is also measured with a horizontally positioned mirror. With the measured diode voltages, the absorptivity coefficient η can be calculated (Conzen et al., 2017):

$$\eta = \left(1 - \frac{U_1}{U_{1C}} - \frac{U_2 - U_1 \cdot \frac{U_{2C}}{U_{1C}}}{U_{2V}}\right) \cdot 100\%$$

η : absorptivity[%]; $U_{1,2}$: diode voltages at measurement [V], $U_{1C,2C,2V}$: diode voltages at calibration [V]

Here U_1 and U_2 correspond to the diode voltages measured during welding, U_{1C} and U_{2C} to the corresponding diode voltages of the calibration measurement with tilted mirror and U_{2V} to the upper diode voltage with a horizontally tilted mirror of the two integrating spheres. The first term ($\frac{U_1}{U_{1C}}$) indicates the radiation measured in the lower integrating sphere reflected by the sample, without taking the vertically reflected radiation into account. The second term describes the proportion of radiation measured in the upper integrating sphere. After correction by the proportion also measured in the lower integrating sphere, this term contains the vertically reflected radiation only. The absorptivity will be used to compare the welding processes between the lasers at 1070 nm, 515 nm and 450 nm wavelength. For those wavelengths, the same measurements are conducted with the change of the wavelength specific components such as beam splitter, filters and mirrors.

Results

Classification of available beam sources (modeling)

In order to obtain a parameter map that shows the accessible process regimes for welds in Cu-ETP and CuSn6 as a function of laser beam parameters, namely laser output power and focal beam diameter, for laser beam sources with a wavelength of 450 nm, calculations based on a linear heat conduction model were performed. Using the formula for the temperature in case of a plane heat source moving on the surface of the workpiece (Carslaw and Jaeger, 2004) maximum temperature values were computed as a function of the laser beam parameters and compared to the liquidus temperatures of both materials in order to determine power thresholds (TH) for the heat conduction welding (HCW) regime as a function of focal diameter. The same procedure is applied to estimate thresholds for deep penetration welding (DPW) based on the boiling point of pure copper at 2595 °C. The heat source is chosen to reflect the intensity distribution of the laser beam and to account for the absorptivity of the material that only allows a portion of the laser intensity to be used for heating the workpiece. The surface conditions (i.e. roughness and degree of oxidation) were considered implicitly by taking the measured absorptivity of 70% at 450 nm (c.f. Fig. 1). For all calculations the focal position was expected to be placed on top of the workpiece. Constant values for the thermophysical material properties were used as they are specified in the respective data sheets at 20 °C (Deutsches Kupferinstitut 2005a, 2005b). Laser beam sources with a wavelength of 450 nm currently available on the market are listed in Table 4.

Their output power ranges between 150 W and 1500 W at fiber diameters from 200 µm to 1000 µm. For the classification of each laser source according to the welding regimes, power in the range of 10% to 100% of the maximum output power and focal diameters according to magnifications between 0.5 and 2 times the fiber diameter are considered. The areas in parameter space covered by these ranges are indicated in Fig. 4 by the corresponding mapping colors.

The resulting process map in Fig. 4 leads to a classification of currently available laser sources with a wavelength of 450 nm. It follows that for Cu-ETP all laser beam sources can be used to perform heat conduction welding. For deep penetration welding only the laser sources with power ≥ 500 W can be used with small focal diameters. For CuSn6 on the other hand, both heat conduction welding and deep penetration welding is possible with a sufficient power density for all available beam sources.

It should be noted that the contour lines separating the process regimes are to be understood as estimates due to the simplifying assumptions of the underlying heat conduction model. In particular, these are: no losses in the optical path of the laser beam, an ideal beam quality factor of 1, no heat losses from the surface, a purely perpendicular incidence of the laser radiation, constant material parameters, no energy sinks due to latent heats, and an ideal contact between the welded parts corresponding to bead-on-plate welds. Furthermore, the results are

Table 4
Commercially available laser beam sources with 450 nm wavelength (Laserline GmbH, 2019; Nuburu Inc, 2019).

laser manufacturer	model	maximum output power	fiber diameter	mapping color
[-]	[-]	P_L [W]	d_F [µm]	[-]
Nuburu	AO-150	150	200	1
Nuburu	AO-500	500	400	2
Laserline	LDMblue500-60	500	600	3
Laserline	LDMblue1000-60	1000	600	4
Laserline	LDMblue1500-100	1500	1000	5

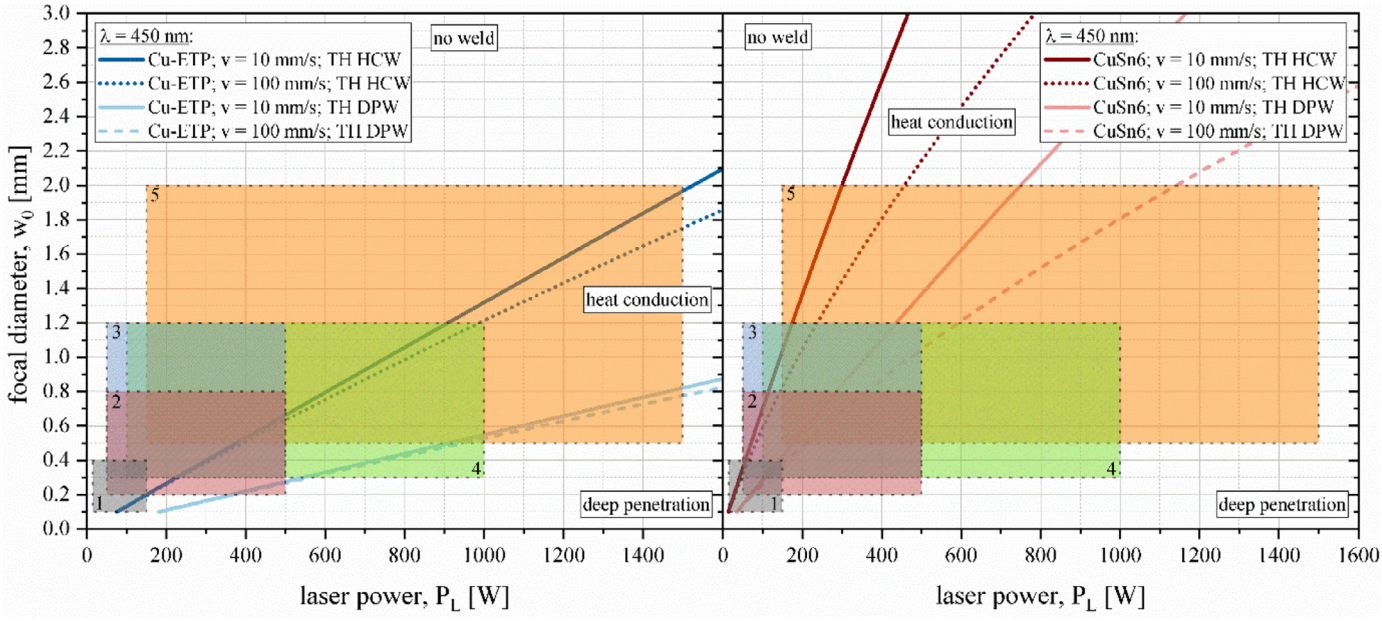


Fig. 4. Laser welding thresholds for 450 nm wavelength for Cu-ETP and CuSn6 including available laser beam sources.

valid only for cases with weld seams much smaller than the workpiece dimensions, since no heat accumulation from the side or bottom faces of the workpiece was accounted for. In a real process these influences may change the power thresholds and would require a revaluation of the parameter map.

Weld depth

For an overview of possible welding depths, bead-on-plate welds are conducted on Cu-ETP and CuSn6. The parameter-dependent process results allow parameter selection for later joint configurations. In this case, the welds are performed on 1 mm thick material samples. The results show the minimum welding depth considering the high thermal mass compared to thinner material samples. For materials with lower layer thickness, it is then possible to select process parameters with suitable penetration depths. The welding depths were obtained by evaluating longitudinal sections along the central axis of the weld seam. It is to be said that for low feed rates < 1 mm/s strong oxidation occurred on both material Cu-ETP and CuSn6 surfaces. In Fig. 5, exemplary longitudinal sections of CuSn6 are shown. An overview of all investigated parameters is illustrated in Fig. 6.

The visible weld seams show a stable penetration depth as soon as an equilibrium state is achieved. The samples show no pore formation inside the weld seam which enables these processes with the laser beam source at 450 nm wavelength as possible candidates for electrical applications. The investigated laser parameters with the welding depths are shown in Fig. 6.

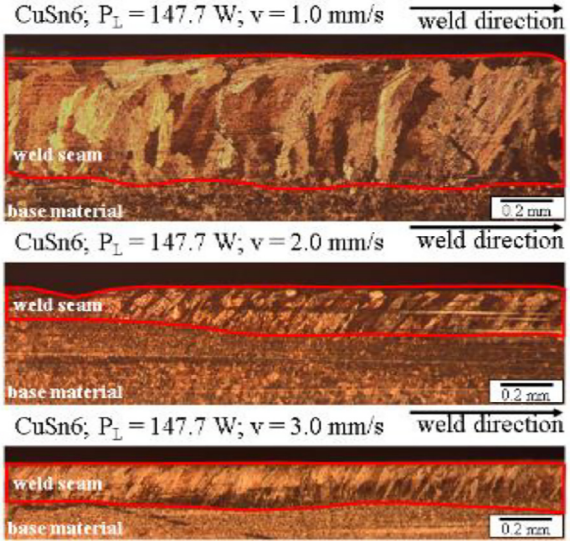


Fig. 5. Longitudinal sections of CuSn6.

With the wavelength of 450 nm and a power of 147.7 W and feed rates from 5 mm/s to 0.1 mm/s welding depths between 100 µm to 648 µm for CuSn6 and 143 µm to 312 µm for Cu-ETP could be achieved. As mentioned before, with feed rates < 1 mm/s strong oxidation oc-

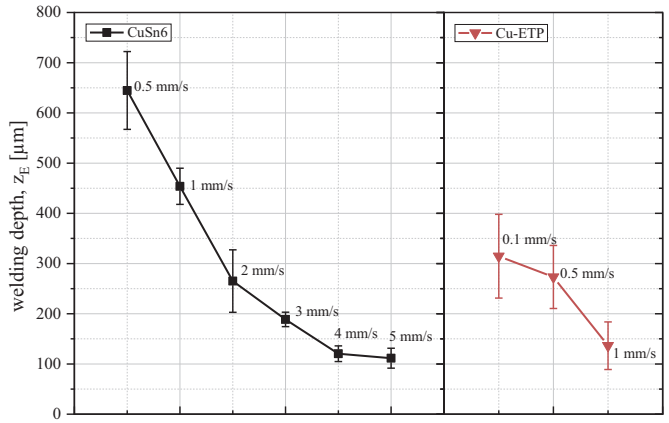


Fig. 6. Welding depth of CuSn6 and Cu-ETP depending on feed rate at constant laser power of 147.7 W (same vertical scale for CuSn6 and Cu-ETP).

curred on the surface. That is why no reproducible weld seams on Cu-ETP can be performed. On CuSn6 however, higher feed rates are possible for the welding process with sufficient penetration depth.

In the high speed videography videos the dynamics during the welding process are observed, as shown in Fig. 7. The video is separated in single pictures, which show examples of important events.

At the beginning of the energy input, a radial interference pattern spreads out on the surface of the material because a temperature gradient in the material is set starting from the welding spot. Further energy input results in a molten pool with impurities on the surface. The photograph shows that these are slaglike agglomerations. In the further course of the welds, these individual particles join together to form a coherent agglomeration. To form the molten pool it takes 0.1 s for CuSn6 and 0.8 s for Cu-ETP. This long exposure time of the material to the laser radiation causes a strong temperature increase in the entire material which leads to oxidation of the material surface. The formation of copper(II)-oxide can be seen from the discoloration and porosity of the surface of the copper sample after welding. Due to the change in the optical properties of the material during the welding process as a result of the strong oxidation on Cu-ETP, the surface shows different optical properties depending on the welding parameters. This results in inhomogeneous and non-reproducible welds for low feed rate <1 mm/s to achieve high penetration depths. The high-speed images clearly show that the laser intensity is not sufficient to ensure energy input for rapid melting of the material due to the high thermal conductivity of the material.

Laser energy absorption

Determining the laser absorption during the process, allows a more detailed insight into the process stability and efficiency. The results in Fig. 8 show the temporal curves of laser absorptivity during the process. Comparing three wavelengths (1070 nm, 515 nm and 450 nm) allows a first estimation on how the laser interacts with the copper material. To the present sate, it is not yet possible to bring all three laser beam sources of different wavelengths to the same focal diameter and perform welding tests in the integrating sphere. This limitation is due to the different designs (fiber laser, disk laser, diode laser) of the laser beam source and the minimum working distance between the focusing optics and the material sample inside the integrating sphere of 150 mm. For this reason, the measurements shown here for heat conduction welding are only a reference points for comparing the wavelengths and should not be regarded as absolute values. The laser power for the 450 nm laser beam source is further reduced on the material surface during the process due to the transmission properties of the beam splitter used for the integrating spheres.

Table 5
Average absorptivity depending on laser parameter for Cu-ETP and CuSn6.

Cu-ETP		
Parameter		Absorptivity
P_L [W]	v [mm/s]	η [%]
131.7	30	72.8 ± 0.83
131.7	10	69.8 ± 0.38
131.7	5	83.1 ± 0.61
131.7	3	82.7 ± 2.2
131.7	1	72.4 ± 0.76
131.7	0.5	83.7 ± 1.04
CuSn6		
Parameter		Absorptivity
P_L [W]	v [mm/s]	η [%]
131.7	30	72.6 ± 3.52
131.7	10	74.9 ± 1.1
131.7	5	74.9 ± 0.38
131.7	3	75.7 ± 0.19
131.7	1	76.6 ± 0.52
131.7	0.5	75.4 ± 1.51

In the left diagram, the baseline welds using a 1070 nm laser source are shown. An average absorptivity between 3% and 10% is measured for both welding parameters. Those values match with the aforementioned values from the spectroscopy. Local fluctuations in the range of ± 3% are visible during the process. The values for the 515 nm laser wavelength show the improved absorptivity during the welding process. For the heat conduction welding process, the average absorptivity for both measurements increases up to 60% while at the same time the local fluctuations decrease to ± 1%. The dark green line at 900 W shows a different behavior at the beginning of the measurement. This phenomena can occur from the extended preheating of the material due to the lower laser power before melting up the material. However, the average absorptivity is determined in the area of the stable, constant welding process. For 450 nm wavelength the measurements show a further increase in the average energy absorption up to 70% to 80%. In this case, the parameters with lower feed rate show a higher absorptivity due to the increased temperature in the material. The variation in the absorptivity measurements for the 450 nm wavelength occur due to an instable process because of the limited laser power. It is possible that the parameter are at the limit of the welding process, although a weld seam is visible on the surface The increased offset from the spectroscopy measurements (Fig. 1) result from increased material temperatures during the process (Blom et al., 2003). At the same time, no local fluctuations within one welding process can be noticed anymore. The average absorptivity for all measured parameters is given in Table 5.

The measurements show a stable absorptivity for CuSn6. For all laser parameters the values vary between 72.6% and 76.6%. Lower feed rate shows a positive influence on the absorptivity within the range of the standard deviation. Regarding the absorptivity on Cu-ETP, the values vary stronger between 69.8% and 83.1% whereas an overall increase in the absorptivity with lower feed rates is recognizable. One possible option for the strong derivation between the parameter could be the five times greater thermal conductivity of Cu-ETP compared to CuSn6. This circumstance together with the low maximum laser power of the laser beam source ensures that no stable equilibrium state can be achieved in the melt pool.

Technical application

After determining the possible welding depths, joint welds are evaluated. Butt and overlap joints are investigated to show the feasibility of scanner based laser micro welding with 450 nm wavelength for technical applications. In this part, only a few laser parameter combinations

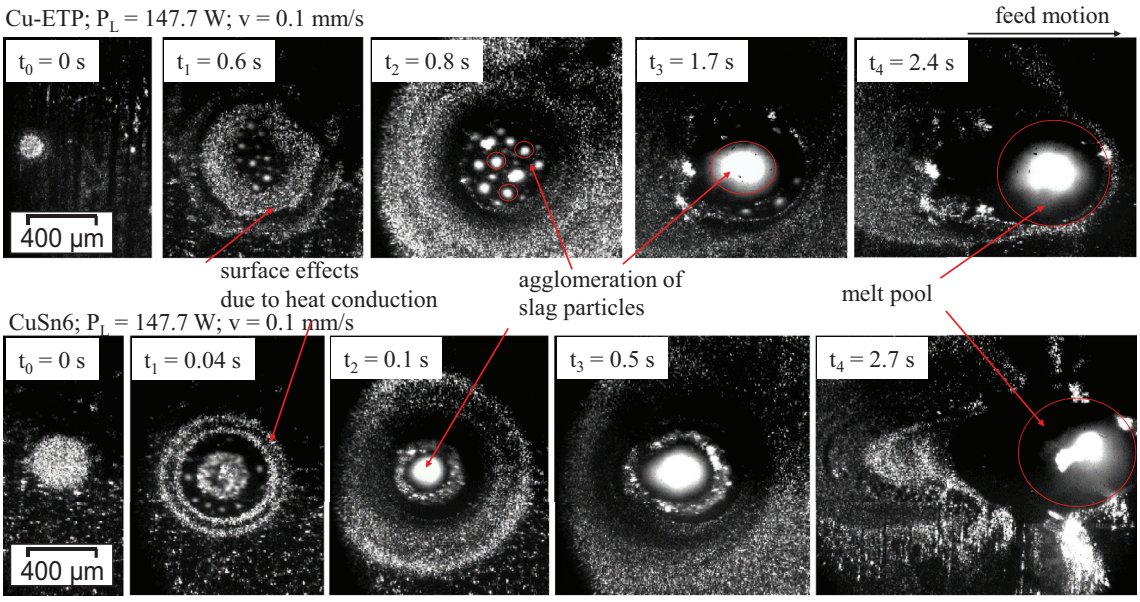


Fig. 7. High speed videography of laser welding processes of Cu-ETP and CuSn6.

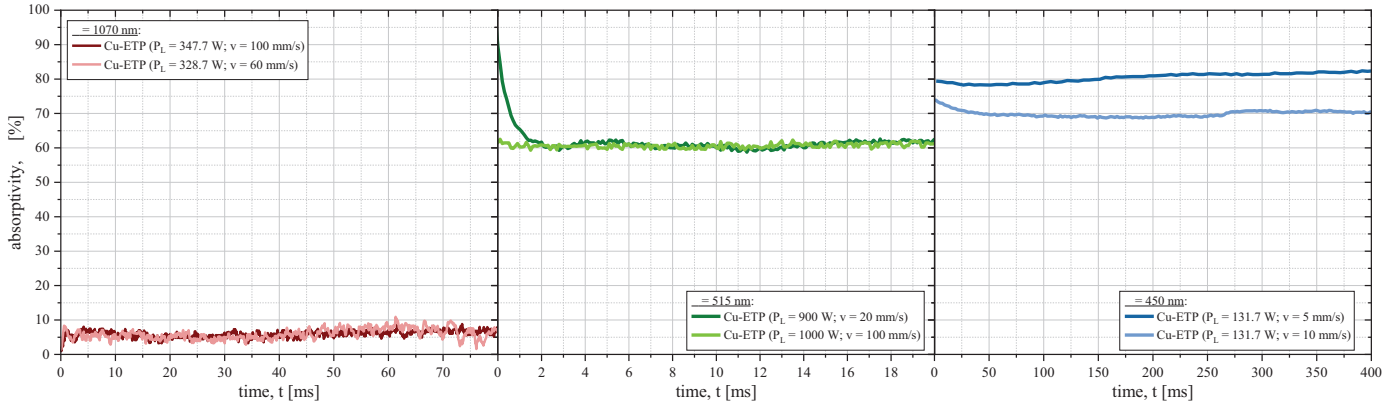


Fig. 8. Absorptivity for heat conduction welding processes at 1070 nm, 515 nm and 450 nm wavelength.

are shown together with the welding results. Due to the gap between the two welding partners with no thermal conductivity in between, the application on Cu-ETP was not possible. The laser power in this case is too low for sufficient energy input to melt up both welding partners. In Fig. 9 the results for CuSn6 are shown.

It is clearly visible, that for both 0.15 mm and 0.3 mm thick material a sufficient connection can be applied. The weld seam quality shows no significant pore formation. For the butt joint of 0.15 mm thick CuSn6 (Fig. 9(a)) the material is fully penetrated and the metallographic cross sections shows the same grain size for the base material and the weld seam. In the overlap configuration of 0.15 mm thick CuSn6 (Fig. 9(b)) a connection could be achieved but there is no complete connection for the two joining partners. The material of the lower layer could not be melted due to the gap and therefore no complete connection could be established. This circumstance prohibits the use of such weld seam for electrical applications. For CuSn6 of 0.3 mm layer thickness a connection could be established as well (Fig. 9(c)). In this case, the penetration depth is about 120 µm magnitude. The material is not completely connected and a gap in the lower part is visible. This gap can be overcome by further reducing the feed rate. With the following parameters in Table 6 weld joints for CuSn6 of different layer thickness could be achieved.

With these parameters the feasibility of scanner based welding with a 450 nm laser beam source for technical applications is shown. It is to

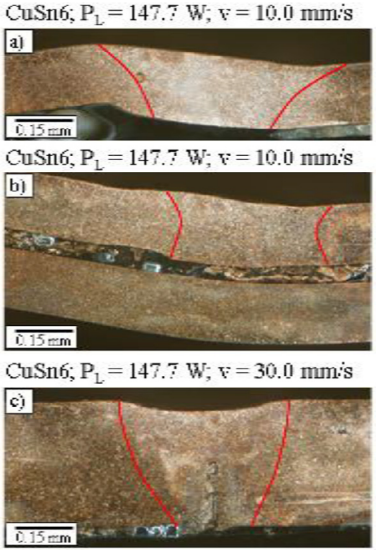


Fig. 9. Joint configurations of CuSn6 (a) butt joint 0.15 mm; (b) overlap joint 0.15 mm (c) butt joint 0.3 mm.

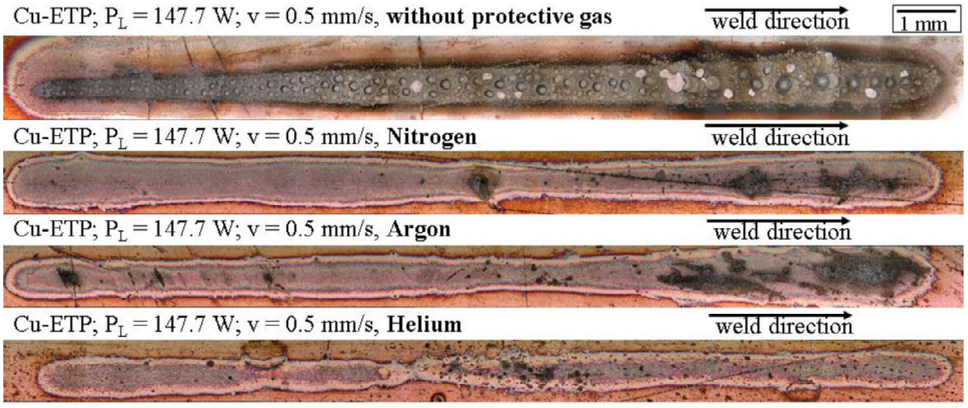


Fig. 10. Influence of protective gases on welding results.

Table 6
Parameters for joining configurations on CuSn6.

CuSn6			
Parameter		Joining configuration	Material thickness
P_L [W]	v [mm/s]	[–]	[mm]
147.7	10	Butt joint	0.5
147.7	30	Butt joint	0.3
147.7	3	Overlap joint	0.3
147.7	50	Butt joint	0.15
147.7	10	Overlap joint	0.15

be kept in mind, that by increasing the laser power or decreasing the feed rate, higher penetration depths can be achieved with a trade off in the surface quality due to stronger oxidation. The different levels of oxidation depending on the material and the laser parameters prohibit the comparison of the surface roughness for the different wavelengths.

Protective gas

Most of the achieved welding depths were only able due to very low welding speeds down to 0.1 mm/s. Continuous weld seams with infrared fiber lasers can be produced using feed rates 10–100 times faster (Häusler et al., 2017). The energy input during these processes is high which leads to strong thermal oxidation. This oxidation reduces the material quality and can lead to uneven weld seams. To avoid oxidation in the process the use of protective gas is additionally investigated to shield the process area from contact with oxygen. For this purpose nitrogen, helium and argon are used to determine the influence on the process result. In Fig. 10 a weld seam with strong oxidation welded without protective gas is shown.

The welding process is executed from the left to the right at first a narrow weld seam is visible, which increases in width as the process progresses. This effect is caused by the increasing heating of the surrounding material, which leads to a widening of the melt pool. When applying a pool of protective gas with a layer thickness of 40 mm a clear change in the process result can be observed. For all three gases an overall reduction of the material penetration can be observed from the top view. The bright areas on the left indicate only a heat affected zone without melting up the material. Proceeding to the right side of the weld seam, partial areas are melted up and oxidize due to the heat accumulation in the material with ongoing process duration. However, a cross section has shown no visible penetration of the material anymore. In these observations, it is particularly noticeable because there is not enough residual power to compensate this influence. It can be concluded, that for a process with a laser beam source at 450 nm wavelength, using protective gases reduces the reproducibility of the welding process. Looking at the spectral data for all three gases provided by the National Institute of Standards and Technology NIST (Kramida and Ralchenko, 2019) no absorption lines from the ground state can be observed for the gases in the region of 450 nm wavelength. In this case, another phenomena than absorption must be the reason like for example cooling of the material surface due to the gas. When using laser beam sources with increased output power, the protective gases can have a positive influence on the surface quality by reducing oxidation.

Conclusions and outlook

In the present work, a feasibility study on a scanner based optical setup with a low power 450 nm diode laser was carried out. The setup was implemented in order to achieve more degrees of freedom in the geometric design of the weld seams than with fixed optics. Additionally a model based comparison of all available laser beam sources to this point was made to give an overview of the possible applications. The results of the investigations are as follows:

i. At the current state, laser beam sources of 450 nm wavelength are available of output power up to 1.5 kW which allows the processing of laser micro welding with heat conduction welding as well as deep penetration welding. In this work, the experimental setup was conducted with the laser beam of lowest power available.
ii. The absorptivity and therefore the energy input during the process increases from 1070 nm to 515 nm and 450 nm wavelength. Local fluctuations during the process decrease which indicates a more stabilized energy input.
iii. With the used experimental setup penetration depths of 648 µm on CuSn6 and 312 µm on Cu-ETP could be achieved.
iv. Strong oxidation at low feed rates prohibit the reproducible joining of Cu-ETP.
v. Butt and overlap joints with CuSn6 for material thicknesses of up to 0.5 mm are possible with higher feed rates and thus better surface quality.

For further investigations a laser beam source of 450 nm wavelength with increased output power will be used to ensure a stable melt pool and to increase the feed rate both on CuSn6 and Cu-ETP. For better comparison of the results of the absorptivity same spot diameters and same laser parameters have to be set up for all different wavelengths which is not possible to the current state. It will also be possible to investigate deep penetration welding with 450 nm wavelength laser beam sources.

Declaration of Competing Interest

The authors declare that they have no known competing financial interests or personal relationships that could have appeared to influence the work reported in this paper.

Acknowledgment

The presented investigations were carried out at RWTH Aachen University within the framework of the Collaborative Research Centre SFB-1120-236616214 “Bauteilpräzision durch Beherrschung von Schmelze und Erstarrung in Produktionsprozessen” and funded by the Deutsche Forschungsgemeinschaft e.V. (DFG, German Research Foundation). The sponsorship and support is gratefully acknowledged.

References

Balck, A., Baumann, M., Malchus, J., Marfels, S., Witte, U., Dinakaran, D., Ocylok, S., Weinbach, M., Bachert, C., Kösters, A., Krause, V., Lell, A., König, H., Stojetz, B., Strauss, U., Löffler, A., Chacko, R.V., 2018. 700 W blue fiber-coupled diode-laser emitting at 450 nm. In: High-Power Diode Laser Technology XVI. SPIE, San Francisco, United States, p. 2 27.01.2018–01.02.2018.

Baumann, M., Balck, A., Malchus, J., Chacko, R.V., Marfels, S., Witte, U., Dinakaran, D., Ocylok, S., Weinbach, M., Bachert, C., Kösters, A., Krause, V., König, H., Lell, A., Stojetz, B., Ali, M., Strauss, U., 2019. 1000 W blue fiber-coupled diode-laser emitting at 450 nm. In: Proceedings of the 2019 High-Power Diode Laser Technology XVII, San Francisco, California, United States, San Francisco, United States, SPIE, Bellingham, Washington, p. 3 3-5 February 2019.

Blom, A., Dunias, P., van Engen, P., Hoving, W., de Kramer, J., 2003. Process spread reduction of laser microspot welding of thin copper parts using real-time control. In: Photon Processing in Microelectronics and Photonics II. SPIE, San Jose, CA, p. 493.

Carslaw, H.S., Jaeger, J.C., 2004. Conduction of Heat in Solids, 2nd ed. Clarendon Press, Oxford.

Conzen, J.H., Häusler, A., Stollenwerk, J., Gillner, A., Poprawe, R., Loosen, P., 2017. Laserstrahl-Mikroschweißen von mikroelektronische Baugruppen unter Anwendung von örtlicher und zeitlicher Energiedeposition. Elektronische Baugruppen und Leiterplatten EBL. Deutscher Verbandfür Schweißen undverwandte Verfahren e.V.

Deutsches Kupferinstitut, Werkstoff-Datenblatt CuSn6 – CW452K (2.1020), 2005a. https://www.kupferinstitut.de.

Deutsches Kupferinstitut, Werkstoff-Datenblatt Cu-ETP – CW004A (2.0065, 2.0060), 2005b. https://www.kupferinstitut.de.

Finuf, M., Ream, S., Gray, B., Pelaprat, J.M., Zediker, M., Fritz, R. (Eds.), 2017. Stable conduction and keyhole welding of copper with 275 watt blue laser. German Scientific Laser Society.

Häusler, A., Mehlmann, B., Olowinsky, A., Gillner, A., Poprawe, R., 2017. Efficient copper microwelding with fibre lasers using spatial power modulation. Lasers Eng. (LIE) 36, 133–146.

Kramida, A., Ralchenko, Y., 2019. NIST Atomic Spectra Database, NIST Standard Reference Database 78. National Institute of Standards and Technology.

Laserline GmbH, Laserline LDMblue: Blue High Power Diode Laser, 2019. https://www.laserline.com/fileadmin/Dokumente/Broschueren_EN/Laserline-LDMblue-product-brochure.pdf (accessed 21 October 2019).

Mehlmann, B., 2014. Spatially modulated laser beam micro welding of CuSn6 and nickel-plated DC04 steel for battery applications. JLMN 9, 276–281.

Moeller, E. (Ed.), 2014. Handbuch Konstruktionswerkstoffe: Auswahl, Eigenschaften, Anwendung, 2nd ed.. Hanser, München.

Nuburu Inc, Nuburu AO Product line. 2019 https://www.nuburu.net/products/ (accessed 21 October 2019).

Wang, H., Kawahito, Y., Yoshida, R., Nakashima, Y., Shiokawa, K., 2017. Development of a high-power blue laser (445 nm) for material processing. Opt. Lett. 42, 2251–2254. https://doi.org/10.1364/OL.42.002251.

Zediker, M.S. (Ed.), High-Power Diode Laser Technology XVI, 2018. Blue laser diode (450 nm) systems for welding copper. SPIE 2018.

Zediker, M.S. (Ed.), Proceedings of the High-Power Diode Laser Technology XVII, 2019. 500 watt blue laser system for welding applications. SPIE, Bellingham, Washington 3-5 February 2019, San Francisco, California, United States.